The Quartz Crystal Microbalance: a Tool for Probing Viscous/Viscoelastic Properties of Thin Films

Mário Alberto Tenan
Centro de Ciências Exatas e de Tecnologia
Universidade de Mogi das Cruzes
08780-911 Mogi das Cruzes, SP, Brazil

and

David Mendes Soares
Instituto de Física 'Gleb Wataghin'
Universidade Estadual de Campinas, Unicamp
13083-970 Campinas, SP, Brazil

Received 29 October, 1998

Techniques based upon the electrical response of the quartz crystal microbalance (QCM) have been widely used in laboratories as routine tools. In this article we present and discuss applications of the QCM (or its variant, the electrochemical quartz crystal microbalance, EQCM) to the viscoelastic characterization of films. It is pointed out that correlations between the motion of quartz crystal and contacting films and overlayers as well as the influence of the electronic circuit on the electric state of the whole system are of fundamental importance in interpreting the results.

I Introduction

Techniques based upon the frequency response of a quartz crystal resonator have been widely used to investigate thin films properties. As a matter of fact, a wealth of physicochemical information on a variety of systems has been obtained in recent years. Good examples are provided by Refs. [1-5]

Devices which comprise a thin AT-cut quartz crystal plate acted on harmonically by an electronic driver are very sensitive to deposition or accumulation of surface mass. Although sensitivity is not restricted to mass changes, this kind of apparatuses is known as quartz crystal microbalance, or QCM for short.

In the late 1950s, Sauerbrey[6] pioneered the quantitative description of the QCM behavior. Taking into account the physical nature of the motion of the crystal resonator, he was able to predict the resonant frequency decrease caused by a thin overlayer. Sauerbrey's formula has become the basis for the interpretation of QCM data concerning film deposition at the gas/solid interface. Later on the understanding of the influence of elastic films on the resonator response was advanced by other authors[7, 8]. The simplified[8] formula for the frequency shift as obtained from the acoustic-wave analysis of a loaded oscillator is currently used in commercial thickness monitors[9]. The use of QCMs has not been restricted to experiments in air or in vacuum. It was verified experimentally[10, 11] that quartz resonators could also respond to properties of a contacting liquid. Those observations opened the way for the investigation of properties of liquids[12, 13] or of films immersed in liquids. Interfacial slip[14], lossy adsorbates[15], film rheology[16], dispersion in colloidal films [17], conductive fluid[18], conducting-polymer films [19], protein multilayers[20], and phase transitions in liquid crystals and lipid multibilayers[21] are only a few examples of the use of QCM to investi-

gate fluids properties.

Impedance/admittance analysis, i. e. the record of the spectrum of electrical impedance/admittance of the compound resonator (crystal plus viscous/viscoelastic media) as a function of the exciting frequency, has changed the focus of study from the physical behavior of the system to its electrical behavior. To this purpose methods based on the Butterworth-van Dyke circuit [22] has been used quite effectively. Basically, the equivalent circuit consists of two branches. One branch contains a simple capacitor to take account of the overall capacitive effects due to (i) the parallel electrodes deposited on the crystal surfaces and (ii) those introduced by external electrical connections. The other branch consists of a series connection of an inductance, a capacitance and a resistance. These components in the series branch (motional arm) of the equivalent circuit are determined by the physical properties of the quartz and of the loading layers, in particular, the series resistance can be interpreted as a measure of mechanical losses in the compound resonator. Based on this equivalent circuit, many researchers have investigated the properties of gases [23], liquids [24-29], interfaces [30], viscoelastic media [31, 32] and sensors [33].

Another electrical analogue description of a layered compound resonator's behavior models the system as a transmission line[34]. Many authors have taken this kind of approach to relate the observed impedance/admittance spectra to overlayer and interface properties [9,35-39].

Although the electrical studies could give valuable contributions to the investigation of film's properties, they can often mask the physical insight into the detailed nature of the loading mechanisms [40, 41]. Models which take into account the correlations between the motion of the quartz and overlayer, as well as the influence of the electronic circuit on the electrical state of the whole system are of fundamental importance in interpreting the results obtained with the help of a QCM [42].

II The Quartz Crystal Microbalance

The QCM consists basically of an AT-cut piezoelectric quartz crystal disc with metallic electrode films deposited on its faces (Fig. 1). One face is exposed to the active medium. A driver circuit applies an ac signal to the electrodes, causing the crystal to oscillate in a shear mode, at a given resonance frequency f_{res}. The quartz crystal microbalance has been routinely used for the determination of mass changes in air or in vacuum (metal-vapor deposition). Measured resonance frequency shifts, Δf_{res}, are converted into mass changes by the well-known Sauerbrey equation[6]. The resonant mechanical oscillations are basically fixed by the crystal thickness, whereas the damping depends on the characteristics of the mounting and the surrounding medium [32]. The use of the QCM in a liquid medium together with electrochemical techniques increased enormously the possibilities of this tool. For this kind of application the microbalance is called the electrochemical quartz crystal microbalance, EQCM. The face in contact with the electrolyte constitutes the working electrode in an electrochemical cell, Fig. 2.

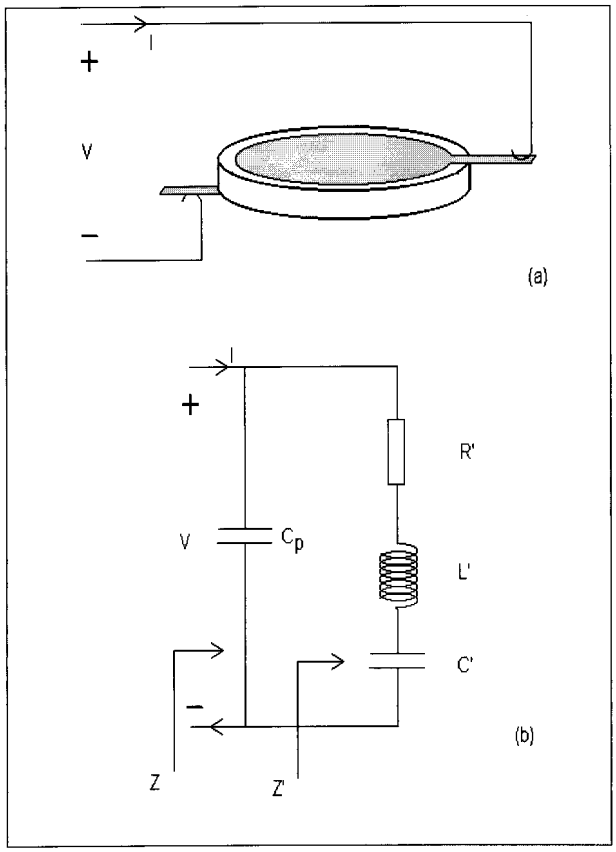

Figure 1. (a) Quartz crystal disk with gold electrode films. (b) Equivalent circuit.

Sinusoidal oscillations occur basically at one of the two modes of the electromechanical resonances corresponding to the crystal equivalent circuit of Fig. 1. These modes are known as the series and the parallel resonant modes (see next Section for details). In a simple mechanical/electrical description, it can be said

that the series-resonant mode depends on the "mass factor" L' and the "spring constant factor" C' of the crystal [42]. At this frequency inductor (capacitance L') and capacitor (capacitance C') are series-resonant and the crystal impedance is essentially resistive (resistance R'). On the other hand, the parallel-resonant mode depends on the mass factor L' and on the capacitance C_P of the electrodes having the crystal as a dielectric. At this frequency the terminal impedance of the crystal is resistive and very high (resistance $>> R'$). To take account of resonances at overtones other RLC series arms should be added in parallel to the $R'L'C'$ branch of Fig. 1.

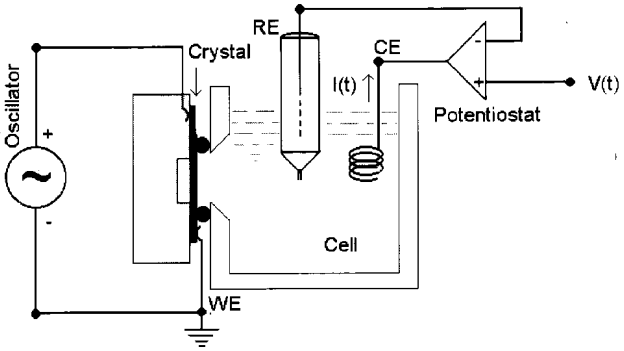

Figure 2. Schematic of an EQCM device. RE: reference electrode, CE: counter electrode and WE: working electrode.

Most QCMs are driven by known oscillator circuits (Pierce, Collpits, Hartley etc.)[43]. Those circuits allow only the monitoring of the resonant frequency changes for low damping media. In a liquid medium, they can be forced to oscillate, but mass change measurements must be correctly interpreted by taking into account the viscous/viscoelastic properties of the medium as shown in Ref. [44].

A nonconventional driver was proposed by Soares [32] for EQCM applications when damping must be taken into consideration during the experiment. It consists of a controlled gain voltage amplifier with positive feedback. The voltage gain being determined by a potentiometer. By increasing the potentiometer resistance P just to the start of oscillations, the amplifier oscillates in the series-resonant mode with $P = R'$ thus allowing the monitoring of both the resonant frequency changes, Δf_{res}, and R' values. Consequently, the power of the modified EQCM [32] resides in its ability of making measurements of viscoelastic properties of films (for example, polymer films and sol-gel phase transformations [39,45,46].

One of the first applications of this setup was to show that Δf_{res} depends on $\Delta R'$. This dependence being related to C_P and to the phase angle added by the driver. Measurements of Δf_{res}, with corrections for $\Delta R'$ were published in Ref.[44], and an application of the modified EQCM for the electrodeposition of polypirrole films can be found in Ref.[47]. It should be stressed that the same dependence should be taken into account when using the conventional oscillator circuits cited above. The main difficulty is that they do not give the value of R', and the corrections for Δf_{res} measurements become impossible.

Conventional use of the EQCM was done for studying double layer structure changes at gold electrodes when no viscoelastic effects were detected. Species in the outer and inner Helmholtz layer, ion solvation and ion pair formation, adsorbed ions, etc., were responsible for the measured frequency shifts[48]. Also the electrodeposition and stripping of CdTe were investigated[49].

III Physical Model

The aim of this section is to present the main points of the model with which one can relate the electrical properties of the resonator to the mechanical properties of the contacting media. Consider a thin transducer plate of thickness d_q with electroded major faces (each of area A) normal to the y-direction (see Fig. 3). If its lateral dimensions are large compared with thickness, the plate can be considered to be laterally infinite in extent. Moreover, for an AT-cut quartz plate one deals with purely thickness-shear propagating waves[50], i.e. owing to the piezoelectric properties and crystalline orientation of the quartz, the application of a voltage between the electrodes results in a shear deformation of the plate. The crystal can be electrically excited into a number of resonant modes (harmonics), each corresponding to a unique standing shear wave pattern across the thickness of the crystal plate (y-direction). One of the resonator's face ($y = 0$) contacts a viscoelastic film of thickness d_f immersed in rather thick layer of a Newtonian liquid, whereas the opposite face ($y = -d_q$) makes contact with air. The oscillating crystal surfaces interact mechanically with the contacting media. Due to the electromechanical coupling that occurs in the quartz the properties of the fluid media are reflected in the electrical properties of the resonator [41, 51].

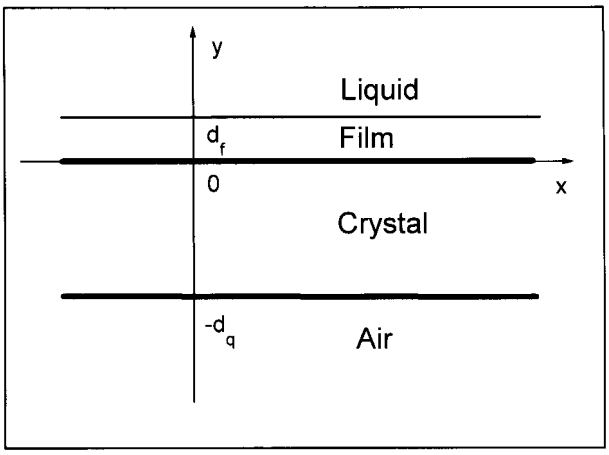

Figure 3. Compound resonator geometry.

The semi-infinite layer of Newtonian liquid is characterized by its density ρ_l and viscosity η_l, and the viscoelastic film by its density ρ_f, shear storage modulus G'_f and viscosity η_f. For quartz we consider the following parameters: density ρ_q, shear modulus c_{66}, piezoelectric constant e_{26} and dielectric constant at constant strain ε_{22}. To take account of dissipation in the quartz plate a phenomenological viscosity η_q[9] can also be considered (its value should be chosen such as to set the quality factor of the unloaded resonator to $\sim 10^5$ [41]).

The behavior of the compound resonator is described in terms of the shear displacement in the x-direction, u_x, which obeys the wave equation

$$\rho \, \frac{\partial^2 u_x}{\partial t^2} = G \, \frac{\partial^2 u_x}{\partial y^2} \; , \qquad (1)$$

where ρ stands for the quartz density (wave propagating in the quartz plate) or the film density (wave propagating in the film), and G, the complex shear modulus, is given by $G \equiv c_{66} + \frac{e_{26}^2}{\varepsilon_{22}} + i \, \omega \, \eta_q$ (wave in the quartz plate) or $G \equiv G_f + i \, \omega \, \eta_f$ (wave in the film). In these definitions, the symbol ω represents the angular frequency of the propagating wave. It should be stressed that the shear modulus G for the quartz plate as defined above comprises the contributions of both the mechanical and electrical properties of the crystal: To derive Eq. (1) for the displacement u_x in the quartz one must take into account the constitutive equations for the piezoelectric material. Those constitutive equations interrelate the electric and the mechanical variables [51].

On the other hand, in the liquid or in air, description is made appropriately in terms of the fluid velocity, $\mathfrak{v}_x$, which obeys the Navier-Stokes equation [52]

$$\rho \frac{\partial \mathfrak{v}_x}{\partial t} = \eta \frac{\partial^2 \mathfrak{v}_x}{\partial^2 y} \; , \qquad (2)$$

with ρ (η) representing density (viscosity) in each fluid.

The solutions of Eq. (1) are obtained for shear waves having a harmonic time-dependence ($e^{i \, \omega \, t}$) and shaped as the superposition of waves travelling in opposite directions. Since the Newtonian fluid layers (liquid and air) are very thick, solutions of Eq.(2), with the same time-dependence $e^{i \, \omega \, t}$, describe perturbations that vanish for large $|y|$ and represent an energy outflow. The solution of the set of Eqs. (1) - (2) for the shear displacement u_x and velocity $\mathfrak{v}_x$ can be determined univocally by imposing the following boundary conditions: (i) vanishing velocity at an infinite distance from the plate, (ii) continuity of velocity at any interface (no-slip condition), (iii)continuity of shear stress across the liquid layer/viscoelastic film interface and (iv) Newton's equation for each electrode which is assumed to be a rigid film of negligible thickness. As a further condition, (v) the electric potential difference across the crystal faces must be equal to the oscillating voltage applied to the electrodes. The current resulting from the application of the voltage can be determined by the time derivative of the electric displacement, which in turn is related to the mechanical variables of the transducer[50]. From a knowledge of the current, the electrical behavior of the compound resonator under impedance/admittance analysis can be derived. It should be stressed that the analysis is purely physical, without use of any electrical analogues.

Some illustrative results of the model are presented in Figs. 4-6, for which the following typical parameters' values were considered: Amplitude of the applied voltage: $V_0 = 1$ V, capacitance of the external connections: $C_{ext} = 10$ pF, 6-MHz crystal plate thickness: $d_q = 0.28$ mm, electrodes area: $A = 0.28$ cm^2, and viscoelastic film thickness and density: $d_f = 1$ μm and $\rho_f = 1$ g/cm^3, respectively. Each electrode was considered to have a thickness $d_e = 200$ nm and a density $\rho_e = 19.3$ g/cm^3 (gold). As typical values for density and viscosity of the Newtonian liquid layer we considered those of water.

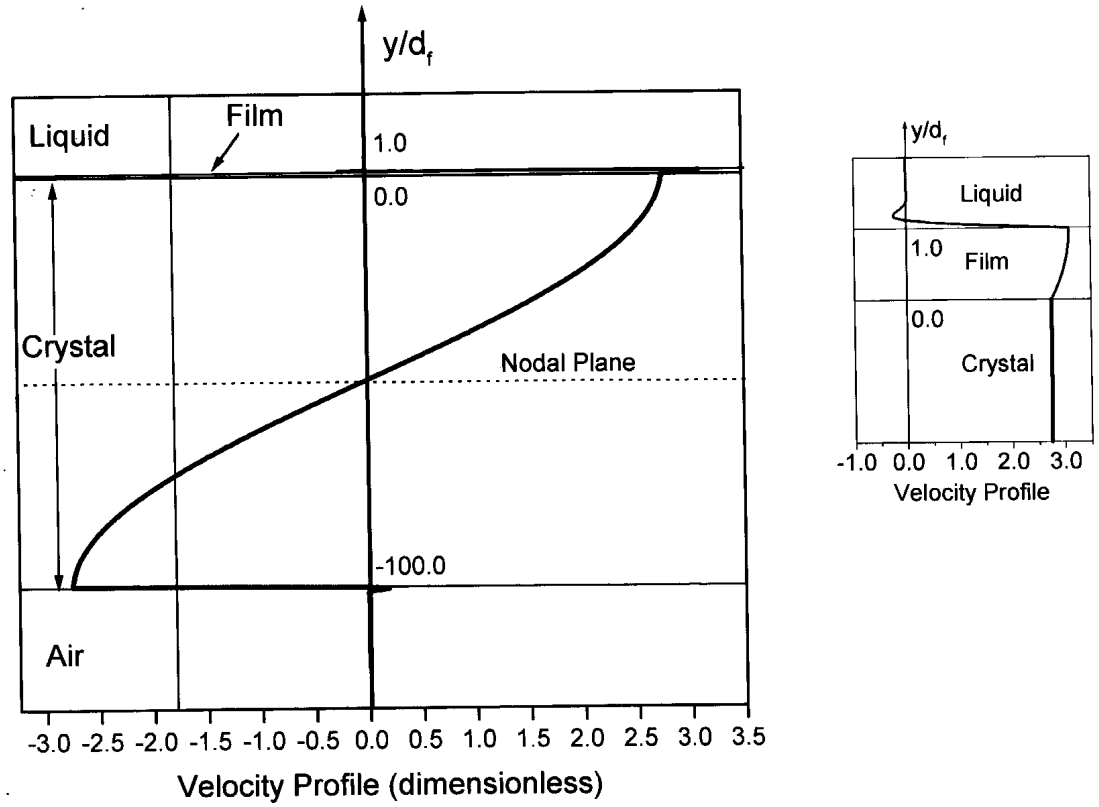

Figure 4. Velocity profile at a time when the disturbance in the quartz plate is a maximum. Inset shows in detail the profile in a small region containing the thin film.

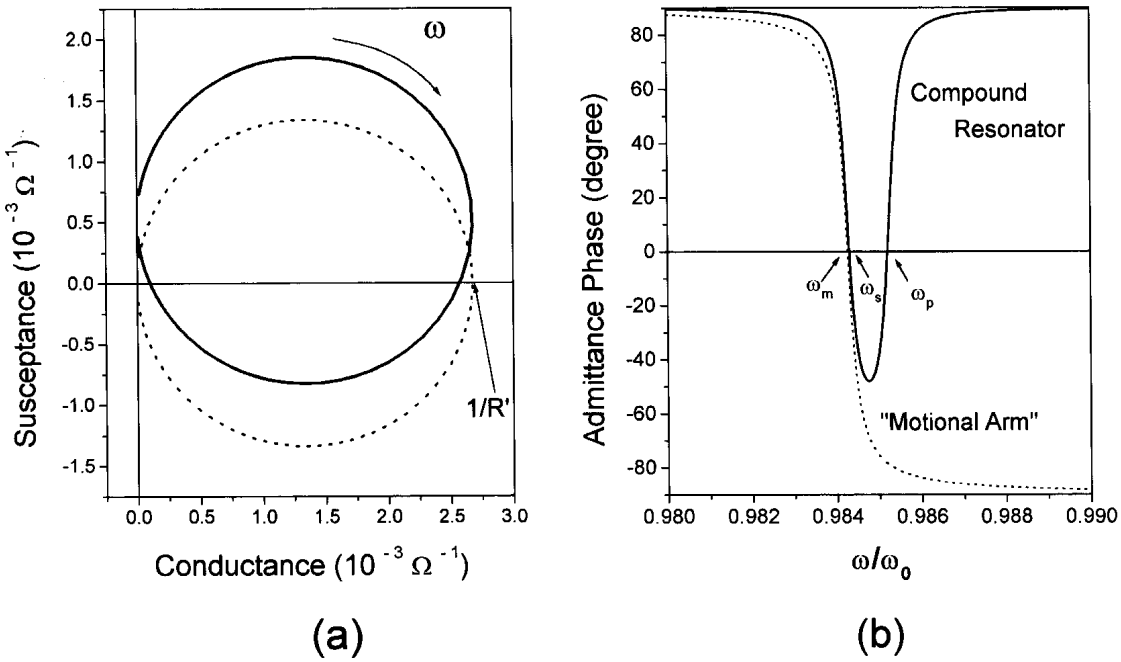

Figure 5. (a) Susceptance-conductance plots in the resonance region. (b) Admittance phase as a function of the exciting frequency ($\omega_0 \cong 3.284 \times 10^7$ rad/s). In (a) and (b), the solid lines refer to the total admittance of the compound resonator, and the dashed lines, to the admittance after subtracting the contributions of the parallel capacitances.

Fig. 4 depicts the shear wave in the compound resonator. The wave is described by the velocity profile at a time when the quartz disturbance is a maximum. In its fundamental mode the crystal plate oscillates back and forth relative to a nodal plane located in the middle region of the plate (dashed line in Fig. 4). A damped shear wave is radiated into the liquid contacting the film and also into the air layer making contact with the opposite crystal face. Inset in Fig. 4 details the wave profile in a small region containing the film.

Model prediction for the electrical behavior of the loaded crystal can be seen in Figs. 5a and 5b. The parametric circle (solid line) in Fig. 5a was obtained by calculating the conductance (real part of the admittance) and the susceptance (imaginary part of the admittance) as functions of the oscillating angular frequency ω. The resulting admittance locus is typical of an electric network containing a capacitance connected in parallel with a $R'L'C'$ series branch [53]. For additional information on the oscillator admittance the reader is referred to the solid line in Fig. 5b, which is a graph of the admittance phase as a function of ω.

If the contributions of the parallel capacitances (external capacitance and electrodes capacitance) are subtracted from the total admittance one obtains the dashed lines in Figs. 5a and 5b. Those curves correspond to the admittance of a RLC series connection. The dashed line in Fig. 5b favors this interpretation: at low frequencies the phase angle tends to $+90^0$, which corresponds to a capacitive admittance, and in the opposite limit the phase angle approaches -90^0, indicating an inductive behavior.

In Fig. 5b three frequencies should be distinguished, namely those at which the admittance phases are zero. At the lowest one (ω_m) the conductance is a maximum ($1/R'$ in Fig. 5a). In terms of the equivalent circuit description ω_m is the frequency at which the motional arm resonates, representing a resonance intrinsic to the mechanical properties of the compound oscillator. The other two frequencies (ω_s and ω_p) correspond to the frequencies at which the susceptance is zero. The susceptance first vanishes at frequency ω_s, which is slightly higher than ω_m. At frequency ω_s the admittance magnitude is virtually a maximum and for this reason it is usually called the "series-resonant " frequency. The susceptance also vanishes at frequency ω_p, for which the admittance magnitude and thus the current are very small, analogous to a parallel resonance [9].

Finally, Fig. 6 illustrates the influence of the mechanical properties of the viscoelastic film on the electrical behavior of the resonator. That figure shows the motional arm resistance R' as a function of the film shear storage modulus G'_f for different values of the film viscosity η_f. Film thickness and density are fixed at 1.0 μm and 1.0 g/cm^3, respectively.

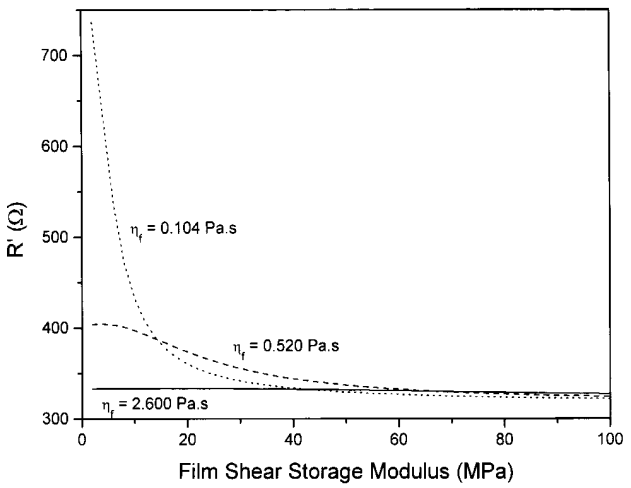

Figure 6. Plots of resistance R' as a function of the shear storage modulus G'_f, for different film viscosities.

The behavior of the viscoelastic film is quite complex, and depends on the interplay between the material's mechanical properties, the shear wavelength and the film thickness. At higher values of the storage shear modulus (G'_f above $\sim$ 80 MPa) the resistance becomes practically independent of the film viscosity; its value ($\sim$320 Ω) is close to that due to the Newtonian liquid overlayer[42]. This behavior is consistent with that of a rigid film that oscillates in phase with the crystal surface. Energy is thus dissipated almost entirely in the contacting liquid medium. Friction within the film contributes very little to the resulting resistance. On the other hand, for 2 MPa $\lesssim G'_f \lesssim$ 10 MPa friction within the film becomes dominant. In this range of values for G'_f the resistance decreases as the film viscosity increases and approaches a limiting value of $\sim$ 320 Ω peculiar to a rigid film in contact with the Newtonian liquid. The prediction that thin films of low viscosity increase considerably the resistance R' is in qualitative agreement with our experimental observations [51].

IV The EQCM as a Sensor for Viscoelastic Changes in Thin Films

As previously discussed, changes of the viscoelastic properties of the quartz contacting phases (liquid and/or film) cause changes of both, L' and R' [46,53,54]. Furthermore, it was shown[25] that changes of the surface morphology of rigid films can also lead to changes of R'

A convenient way to monitor the measured parameters changes during an experiment is to use the impedance plane $Z = \Delta R + i\ \Delta X$, where $\Delta X = 2\pi\ f_{res}\ \Delta L'$ [46]. The relationship $2\ L'\ \Delta f_{res} = f_{res}\ \Delta L'$ [42] allows us to use resonant frequency changes instead of the parameter change $\Delta L'$ in the imaginary axis of the impedance plane. Since R' causes an additional frequency shift, results of frequency measurements can not be related straightforwardly to mass changes. The effect depends on the type of the driver used [32]. Thus it is necessary to obtain previously the calibration curve of the EQCM in the Z-plane. This can be done by plotting the observed Δf_{res} and $\Delta R'$ for known Newtonian fluids (air as a reference system, water, and aqueous sucrose solutions, for example). As $4L'\ \Delta f_{res}/\Delta R = 1$, a 45^0-slope line is obtained in the impedance plane[42]. The difference between the measured values and the expected 45^0-slope line constitutes the calibrating curve (circle). To remove the driver contribution any frequency measurement should be subtracted from the calibrating circle ordinates. Deviations from the 45^0-slope line represent the non-Newtonian properties of the fluid overlayers.

A thin viscoelastic film in contact with a liquid affects the crystal through its acoustical impedance Z_A (ratio of shear stress to surface velocity) at the crystal/film interface. The corresponding electrical impedance can be calculated by: $Z = Z_A/\kappa^2$, where κ is the crystal electromechanical constant [42]. As shown in Ref. [55], the EQCM impedance change is given approximately by the sum of the acoustic impedances Z_F (film impedance) and Z_L (liquid layer impedance), each multiplied by a term representing phase shift and attenuation in the corresponding layer. This holds in the following cases: (i) when $|Z_L| << |Z_F|$, i. e. the film rigidity is much higher than that of the solution layer; (ii) when the film is rigid or (iii) very thin.

The conditions given above were fulfilled in a recent experiment for monitoring a sol-gel phase change from aqueous silicates (Si(OH)4) [56]. Two processes were observed in sequence. First occurred the formation of a thin rigid layer (mass: 2 μg) and then a gradual increase of R' and ΔX ($\Delta R = 75\ \Omega$ and $\Delta X = 38\ \Omega$) indicating a viscoelastic non-Newtonian behavior of the solution adjacent to the silica film. As the processes observed were not simultaneous, the additivity of the impedances allowed us to identify the contributions of the processes taking place within a forming film and those in the solution overlayer.

Finally, it is worth mentioning a technique which gives directly the crystal parameter values [57]. It uses a voltage controlled oscillator to sweep the frequency of the current applied to the crystal. By fitting the resulting potential, the parameters are calculated allowing to make impedance plots of the experiments in real time. This method works as an impedance analyzer. It is a powerful technique but much more expensive than the modified EQCM. It is a recent development and till now not widely used.

V Concluding Remarks

QCM and EQCM have been widely used to investigate properties of liquids or films immersed in liquids. Techniques based on this kind of apparatus have revealed to be valuable tools for investigations of problems such as dispersion in colloidal films, conductive fluids, conducting-polymer films, protein multilayers, phase transitions in liquid crystals, and sol-gel transitions. The key point of the preceding Sections is that caution must be exercised when interpreting the results. Many of the EQCM responses in a variety of situations have yet to be studied and clarified. To this purpose an EQCM should be able to measure the two parameters: Δf_{res} and $\Delta R'$.

VI Acknowledgments

Financial support provided by FAPESP, CNPq and FAEP/OMEC are acknowledged.

References

[1] J. S. Gordon and D. C. Johnson, J. Electroanal. Chem. **365**, 267 (1994).

[2] I. C. Faria, R. Torresi and A. Gorenstein, J. Electroanal. Chem. **38**, 2765 (1993).

[3] G. Inselt and J. Bacskai, Electrochim. Acta **37**, 647 (1992).

[4] V. Tsionsky L. Daikhin and E. Gileadi, J. Electrochem. Soc. **L233**, 142 (1995).

[5] G. Hayward, Anal. Chim. Acta **264**, 23 (1992).

[6] G. Sauerbrey, Z. Phys. **155**, 206 (1959).

[7] J. G. Miller and D. I. Bolef, J. Appl. Phys. **39**, 5815 (1968).

[8] C. Lu and O. Lewis, J. Appl. Phys. **43**, 4385 (1972).

[9] C. E. Reed, K. K. Kanazawa and J. H. Kaufman, J. Appl. Phys. **68**, 1993 (1990).

[10] T. Nomura and A. Minemura, Nippon Kagaku Kaishi **1980**, 1621 (1980).

[11] P. L. Konash and G. J. Bastiaans, Anal. Chem. **52**, 1929 (1980).

[12] H. E. Hager, Chem. Engin. Commun. **43**, 25 (1986).

[13] F. Eggers and Th. Funck, J. Phys. E **20**, 523 (1987).

[14] J. Krim and A. Widom, Phys. Rev. B **38**, 12184 (1988).

[15] Yong-gui Dong, Guan-ping Feng and Cheng-qun Gui, Sens. Actuat. **13-14**, 551 (1993).

[16] H. Muramatsu, X. Ye and T. Ataka, J. Electroanal. Chem. **347**, 247 (1993).

[17] J. S. Graham and D. R. Rosseinsky, J. Chem. Soc. , Faraday Trans. **90**, 3657 (1994).

[18] S. Bruckenstein, M. Michalski, A. Fensore, Z. Li and A. R. Hillman, Anal. Chem. **66**, 1847 (1994).

[19] H. Daifuku, T. Kawagoe, N. Yamamoto, T. Ohsaka and N. Oyama, J. Electroanal. Chem. **274**, 313 (1989).

[20] J. Rickert, A. Brecht and W. Gopel, Anal. Chem. **69** , 1441 (1997).

[21] Y. Okahata and H. Ebato, Anal. Chem. **61**, 2185 (1989).

[22] K. S. Van Dyke, Proc. IRE **16**,742 (1928).

[23] M. Rodahl, F. Hook, A. Krozer, P. Brzezinski and B.Kasemo, Rev. Sci. Instrum. **66**, 3924 (1995).

[24] Ref. 18 kanazawa- H. Muramatsu, E. Tamiya and I. Karube, Anal. Chem. **60**, 2142 (1988).

[25] R. Beck, U. Pitterman and K. G. Weil, Ber. Bunsenges. Phys. Chem. **92**, 1363 (1988).

[26] C. Barnes, Sens. Actuat. **30**, 197 (1992).

[27] Z. Lin, C. M. Yip, I. S. Joseph and M. D. Ward, Anal. Chem. **65**, 1546 (1993).

[28] M. Yang M. Thompson, Anal. Chem. **65**, 1158 (1993).

[29] Z. Shana and F. Josse, Anal. Chem. **66**, 1955 (1994).

[30] M. Yang, M. Thompson and W. C. Duncan-Hewitt, Langmuir **9**, 802 (1993).

[31] T. Okajima, H. Sacurai, N. Oyama, K. Tokuda and T. Oshaka, Electrochim. Acta **6**, 747 (1993).

[32] D. M. Soares, Meas. Sci. Technol. **4**, 549 (1993).

[33] J. Wang, M. D. Ward R. C. Ebersole and R. P. Foss, Anal. Chem. **65**, 2553 (1993).

[34] E. Benes, J. Appl. Phys. **56**, 608 (1984).

[35] T. Nakamoto and T. Moriizumi, Japan. J. Appl. Phys. **29**, 963 (1990).

[36] D. Johannsmann, K. Mathauer, G. Wegner and W. Knoll, Phys. Rev. B **46**, 7808 (1992).

[37] F. Josse, Z. Shana, C. E. Radtke and D. T. Haworth, IEEE Trans. UFFC **37**, 359 (1990).

[38] R. Lucklum, C. Behling, R. W. Cernosek and S. J. Martin, J. Appl. Phys. D **30**, 346 (1997).

[39] H. L. Bandey, A. R. Hillman, M. J. Brown and S. J. Martin, Faraday Discuss. **107**, 105 (1997).

[40] G. Hayward and M. N. Jackson, IEEE Trans. UFFC **33**, 41 (1986).

[41] K. K. Kanazawa, Faraday Discuss. **107**, 77 (1997).

[42] D. M. Soares, M. A. Tenan and S. Wasle, Electrochim. Acta **44**, 263 (1998).

[43] R. J. Matthys, *Crystal Oscillator Circuits*, John-Wiley & Sons, New York, 1984.

[44] C. Fruböse, K. Doblhofer and D. M. Soares, Ber. Bunsenges. Phys. Chem. **97**, 475 (1993).

[45] D. M. Soares, C. A. Bertran and G. P. Thim, Proc. 45th Annual Meeting - International Society of Electrochemistry, p. VII-116, Porto, Portugal (1994).

[46] E. J. Calvo, R. Etchenique, P. N. Bartlett, K. Singhal and C. Santamaria, Faraday Discuss. **107,** 141 (1997).

[47] D. M. Soares, W. Kautek, C. Fruböse and Doblhofer, Ber. Bunsenges. Phys. Chem. **98**, 219 (1994).

[48] W. Kautek, M. Sahre and D. M. Soares, Ber. Bunsenges. Phys. Chem. **99**, 667 (1995).

[49] J. G. N. Matias, J. F. Juliao, D. M. Soares and A. Gorenstein, J. Electroanal. Chem. **431**, 163 (1997).

[50] *Physical Acoustics - Principles and Methods*, edited by W. P. Mason, Vol. I - Part A, Academic Press, New York, 1964.

[51] M. A. Tenan and D. M. Soares, to be published.

[52] G. K. Batchelor, *An Introduction to Fluid Dynamics*, Cambridge University Press, Cambridge, 1967.

[53] D. A. Buttry and M. D. Ward, Chem. Rev. **92**, 1355 (1992).

[54] R. Beck, U. Pitterman and K. G. Weil, J. Electrochem. Soc. **132**, 453 (1992).

[55] V. E. Granstaff and S. J. Martin, J. Appl. Phys. **75**, 1319 (1994).

[56] P. T. Lima, C. A. Bertran and D. M. Soares, 49th Annual Meetring - International Society of Electrochemistry, p. 181, Kytakyushu, Japan (1998).

[57] E. J. Calvo, C. Danilowicz and R. Etchenique, J. Chem. Soc. Faraday Trans. **91**, 4083 (1995).